Articles

Formation and Properties of a Novel Dinuclear, Cationic α-Diimine Palladium-Based Ethylene Polymerization Catalyst Containing a Pd−Pd Bond and Bridging Methylene and Methyl Groups

John H. Brownie and Michael C. Baird*

Department of Chemistry, Queen's University, Kingston, Ontario, Canada K7L 3N6

Lev N. Zakharov and Arnold L. Rheingold

Department of Chemistry, University of Delaware, Newark, Delaware 19716

Received August 19, 2002

The compound $PdMe_2(N\wedge N)$ ($N\wedge N$ = ArN═CMeCMe═NAr, Ar = 2,6-$C_6H_3(i\text{-}Pr)_2$) reacts with the methide abstractors $B(C_6F_5)_3$, $[Ph_3C][B(C_6F_5)_4]$, and $[Ph_3C][CF_3SO_3]$ in the absence of ethylene to give the metal−metal-bonded, dinuclear, cationic complex $[(N\wedge N)Pd(\mu\text{-}CH_2)(\mu\text{-}Me)Pd(N\wedge N)]^+$, which is characterized by ^1H and $^{13}C\{^1H\}$ NMR spectroscopy, mass spectrometry, and X-ray crystallography. This cationic complex, with the three counteranions, reacts with ethylene to produce the same type of low-density polyethylene produced by the known catalyst $[PdMe(solvent)(N\wedge N)]^+$, formed by methide abstraction from $PdMe_2(N\wedge N)$ by $[H(Et_2O)_2][B\{3,5\text{-}C_6H_3(CF_3)_2\}_4]$. Indeed, reaction of the dinuclear species with ethylene results in conversion to the mononuclear $[PdMe(solvent)(N\wedge N)]^+$, which appears to be the true catalytic species. The three weakly coordinating counteranions $[BMe(C_6F_5)_3]^-$, $[B(C_6F_5)_4]^-$, and $[B\{3,5\text{-}C_6H_3(CF_3)_2\}_4]^-$ differ little in their effects on the polymerization process, results consistent with the resting state for this catalytic system being the cationic ethylene complex $[Pd(\eta^2\text{-}C_2H_4)(\sim\text{polymer})(N\wedge N)]^+$. Interestingly, activation by $[Ph_3C][CF_3SO_3]$ gives a catalyst of considerably reduced potency, suggesting that the triflate anion is a better ligand in this system and does compete effectively for the active site on the metal.

Recent reports by Brookhart et al. of the use of aryl-substituted α-diimine Ni(II) and Pd(II) catalysts for the Ziegler−Natta polymerization of alkenes have initiated intense interest in this area of catalysis.[1,2] The catalysts of interest, of the general type shown in Figure 1, are formed by addition of 1 equiv of the strong acid $[H(Et_2O)_2][B\{3,5\text{-}C_6H_3(CF_3)_2\}_4]$ to precursors of the type $PdMe_2(N\wedge N)$ ($N\wedge N$ = aryl-substituted α-diimine); one methyl group is removed as methane (eq 1).[1]

$$PdMe_2(N\wedge N) + [H(Et_2O)_2][B\{3,5\text{-}C_6H_3(CF_3)_2\}_4] \rightarrow [PdMe(OEt_2)(N\wedge N)]^+ + [B\{3,5\text{-}C_6H_3(CF_3)_2\}_4]^- + CH_4 \quad (1)$$

Key features of this type of catalyst are the presence of a methyl ligand cis to a labile ether ligand and the weakly coordinating counteranion $[B\{3,5\text{-}C_6H_3(CF_3)_2\}_4]^-$. The mechanism of the polymerization process has been much studied,[1,3] and experimental evidence points inter alia to a resting state in which an olefin is coordinated to the active site of the catalyst (Figure 2).[1] This is in contrast to many early-transition-metal metallocene

* To whom correspondence should be addressed. E-mail: bairdmc@chem.queensu.ca. Fax: (613) 533-6669.

(1) (a) Johnson, L. K.; Killian, C. M.; Brookhart, M. *J. Am. Chem. Soc.* **1995**, *117*, 6414. (b) Killian, C. M.; Tempel, D. J.; Johnson, L. K.; Brookhart, M. *J. Am. Chem. Soc.* **1996**, *118*, 11664. (c) Johnson, L. K.; Mecking, S.; Brookhart, M. *J. Am. Chem. Soc.* **1996**, *118*, 267. (d) Mecking, S.; Johnson, L. K.; Wang, L.; Brookhart, M. *J. Am. Chem. Soc.* **1998**, *120*, 888. (e) Ittel, S. D.; Johnson, L. K.; Brookhart, M. *Chem. Rev.* **2000**, *100*, 1169. (f) Arthur, S. D.; Bennett, A. M. A.; Brookhart, M. S.; Coughlin, E. B.; Feldman, J.; Ittel, S. D.; Johnson, L. K.; Killian, C. M.; Kreutzer, K. A. U.S. Patent 5866663, Feb 2, 1999, to DuPont (polymerizations). (g) Brookhart, M. S.; Ittel, S. D.; Johnson, L. K.; Killian, C. M.; Kreutzer, K. A.; McCord, E. F.; McLain, S. J.; Tempel, D. J. U.S. Patent 5880241, May 3, 1999, to DuPont (polymer compositions). (h) Brookhart, M. S.; Johnson, L. K.; Killian, C. M.; Wang, L.; Yang, Z.-Y., U.S. Patent 5880323, March 9, 1999, to DuPont (R-olefins). (i) Arthur, S. D.; Bennett, A. M. A.; Brookhart, M. S.; Coughlin, E. B.; Feldman, J.; Ittel, S. D.; Johnson, L. K.; Killian, C. M.; Kreutzer, K. A.; Parthasarathy, A.; Tempel, D. J. U.S. Patent 5886224, March 23, 1999, to DuPont (ligand compositions). (j) Arthur, S. D.; Brookhart, M. S.; Johnson, L. K.; Killian, C. M.; McCord, E. F.; McLain, S. J. U.S. Patent 5891963, April 6, 1999, to DuPont (copolymers).

(2) Möhring, V. M.; Fink, G. *Angew. Chem., Int. Ed. Engl.* **1985**, *24*, 1001.

10.1021/om020673l CCC: $25.00
Publication on Web 12/05/2002

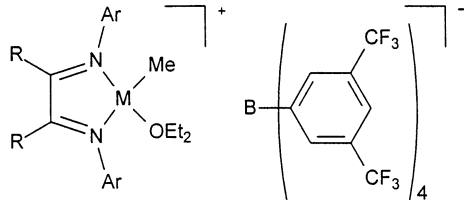

Figure 1. Conventional late-transition-metal ethylene polymerization catalysts (M = Ni, Pd; R = H, Me; Ar = substituted phenyl).

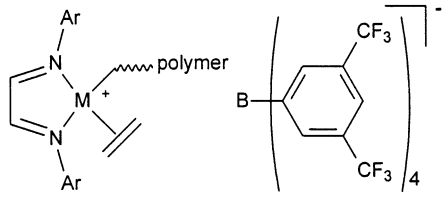

Figure 2. Catalyst resting state for palladium-based catalysts.

systems, where the resting state involves the coordination of the anion to the active site with the result that the coordinating behavior of the counteranion has considerable influence on both the activity of the catalysts and the properties of the polymers obtained.[4,5]

While a great deal of research has focused on the effects of modifying the cationic and the anionic components of early-transition-metal polymerization catalysts,[6] relatively little has been done with respect to the counteranions of late-transition-metal systems.[1,7] Macchioni et al. have investigated the influence of several anions on copolymerizations of styrene and carbon monoxide using a Pd(II) bipyridyl complex,[8] finding that the anions $[B\{3,5\text{-}C_6H_3(CF_3)_2\}_4]^-$, SbF_6^-, PF_6^-, and BF_4^- were little different but that $CF_3SO_3^-$ greatly hindered polymerization. To date, however, no reports have examined anion effects in α-diimine Pd(II) catalyst systems, and we therefore undertook a study of a series of such catalysts containing various counteranions.

(3) (a) Shultz, L. H.; Brookhart, M. *Organometallics* **2001**, *20*, 3975. (b) Tempel, D. J.; Johnson, L. K.; Huff, R. L.; White, P. S.; Brookhart, M. *J. Am. Chem. Soc.* **2000**, *122*, 6686. (c) Shultz, L. H.; Tempel, D. J.; Brookhart, M. *J. Am. Chem. Soc.* **2001**, *123*, 11539.

(4) Bochmann, M. *J. Chem. Soc., Dalton Trans.* **1996**, 255.

(5) See, for instance: (a) Chen, E. Y. X.; Marks, T. J. *Chem. Rev.* **2000**, *100*, 1391. (b) Rappé, A. K.; Skiff, W. M.; Casewit, C. J. *Chem. Rev.* **2000**, *100*, 1435. (c) Lohrenz, J. C. W.; Bühl, M.; Weber, M.; Thiel, W. *J. Organomet. Chem.* **1999**, *592*, 11. (d) Vanka, K.; Chan, M. S. W.; Pye, C. C.; Ziegler, T. *Organometallics* **2000**, *19*, 1841. (e) Chan, M. S. W.; Ziegler, T. *Organometallics* **2000**, *19*, 5182. (f) Lanza, G.; Fragalà, I. L.; Marks, T. J. *Organometallics* **2001**, *20*, 4006. (g) Nifant'ev, I. E.; Ustynyuk, L. Y.; Laikov, D. N. *Organometallics* **2001**, *20*, 5375. (h) Vanka, K.; Ziegler, T. *Organometallics* **2001**, *20*, 905.

(6) For useful reviews see: (a) Möhring, P. C.; Coville, N. J. *J. Organomet. Chem.* **1994**, *479*, 1. (b) Gupta, V. K.; Satish, S.; Bhardwaj, I. S. *J. Macromol. Sci., Rev. Macromol. Chem. Phys.* **1994**, *C34*, 439. (c) Brintzinger, H. H.; Fischer, D.; Mülhaupt, R.; Rieger, B.; Waymouth, R. M. *Angew. Chem., Int. Ed. Engl.* **1995**, *34*, 1143. (d) Bochmann, M. *J. Chem. Soc., Dalton Trans.* **1996**, 255. (e) Kaminsky, W.; Arndt, M. *Adv. Polym. Sci.* **1997**, *127*, 143. (f) Alt, H. G.; Köppl, A. *Chem. Rev.* **2000**, *100*, 1205. (g) Coates, G. W. *Chem. Rev.* **2000**, *100*, 1223. (h) Resconi, L.; Cavallo, L.; Fait, A.; Piemontesi, F. *Chem. Rev.* **2000**, *100*, 1253. (i) Angermund, K.; Fink, G.; Jensen, V. R.; Kleinschmidt, R. *Chem. Rev.* **2000**, *100*, 1457. (j) Scheirs, J., Kaminsky, W., Eds. *Metallocene-based Polyolefins*; Wiley: Chichester, U.K., 1999.

(7) (a) Gates, D. P.; Svejda, S. A.; Oñate, E.; Killian, C. M.; Johnson, L. K.; White, P. S.; Brookhart, M. *Macromolecules* **2000**, *33*, 2320. (b) Michalak, A.; Ziegler, T. *Organometallics* **1999**, *18*, 3998. (c) Michalak, A.; Ziegler, T. *Organometallics* **2000**, *19*, 1850.

(8) Macchioni, A.; Bellachioma, G.; Cardaci, G.; Travaglia, M.; Zuccaccia, C.; Milani, B.; Corso, G.; Zangrando, E.; Mestroni, G.; Carfagna, C.; Formica, M. *Organometallics* **1999**, *18*, 3061.

Scheme 1. Activation of 1 by Methide Abstraction Reactions To Give Cationic Catalysts Containing the Counteranions $[BMe(C_6F_5)_3]^-$ (1-A), $[B(C_6F_5)_4]^-$ (1-B), and $[CF_3SO_3]^-$ (1-C) (S = Solvent)

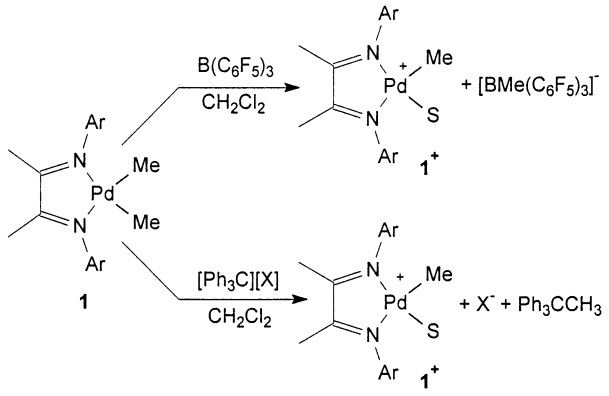

To examine the effects of the anions $[BMe(C_6F_5)_3]^-$, $[B(C_6F_5)_4]^-$, and $[CF_3SO_3]^-$ on the polymers produced, we activated the compound $PdMe_2(N\wedge N)$ ($N\wedge N$ = ArN=CMeCMe=NAr, Ar = 2,6-$C_6H_3(i\text{-}Pr)_2$)[1a] with the methide abstractors $B(C_6F_5)_3$, $[Ph_3C][B(C_6F_5)_4]$, and $[Ph_3C][CF_3SO_3]$, anticipating formation of the conventional cationic, monomethyl palladium complex $[PdMe(solvent)(N\wedge N)]^+$ as in Scheme 1. Instead we obtained the unprecedented, metal−metal-bonded, dinuclear, cationic complex $[(N\wedge N)Pd(\mu\text{-}CH_2)(\mu\text{-}Me)Pd(N\wedge N)]^+$, with bridging methylene and methyl units. We report here the synthesis and characterization (NMR, MS, X-ray) of this novel complex, in addition to its properties as an ethylene polymerization catalyst precursor.

Results and Discussion

Reactions of 1 with Methyl-Abstracting Species. Reactions of **1** in CD_2Cl_2 with an equimolar amount of $B(C_6F_5)_3$, $[Ph_3C][B(C_6F_5)_4]$, or $[Ph_3C][CF_3SO_3]$ resulted in all cases in effervescence and the formation of a deep red solution. We anticipated that the reactions would proceed with 1:1 stoichiometries and that the ^{1}H NMR spectra would exhibit the resonances of the solvated cation $[PdMe(CH_2Cl_2)(N\wedge N)]^+$, including a Pd−Me resonance (3H), two α-diimine backbone methyl resonances (total of 6H relative to Pd−Me), and two isopropyl methyl resonances (total of 24H relative to Pd−Me).[1a] However, NMR monitoring of the reactions of **1** with equimolar amounts of $B(C_6F_5)_3$ and $[Ph_3C][B(C_6F_5)_4]$ indicated that only 0.5 equiv of each activator actually reacted. For instance, with $B(C_6F_5)_3$, a ^{19}F NMR spectrum of the reaction mixture revealed the presence of equal amounts of $B(C_6F_5)_3$ and $[BMe(C_6F_5)_3]^-$, while a ^{1}H NMR spectrum showed that **1** had completely reacted but that only half of the expected amount of $[BMe(C_6F_5)_3]^-$ had formed. The expected Pd−Me resonance (3H) was observed, but the pair of α-diimine backbone methyl resonances were integrated for a total of 12 hydrogen atoms (relative to Pd−Me), while the isopropyl methyl resonances were integrated in total to 48 hydrogen atoms (relative to Pd−Me). Further inspection of the ^{1}H NMR spectrum also revealed a two-hydrogen resonance at δ 5.72 and a methane resonance at δ 0.21, explaining the pronounced effervescence observed in the initial stages of the reaction.

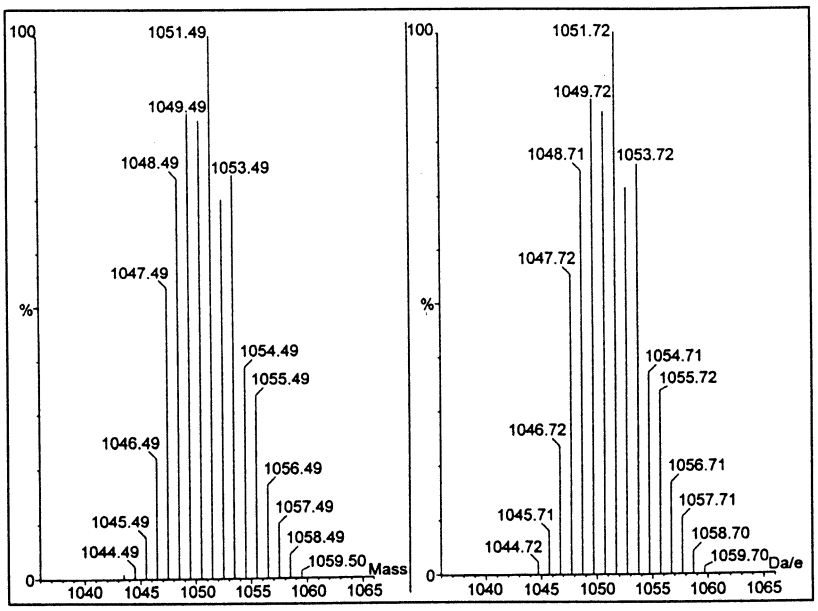

Figure 3. Calculated isotope distribution for $C_{58}H_{85}N_4Pd_2$ (left) (intensity (%) vs mass) and ESMS positive ion spectrum of **2-A** (right) (intensity (%) vs charge-to-mass ratio (Da/e)).

Scheme 2. Possible Route to and Structure of Dipalladium Species 2

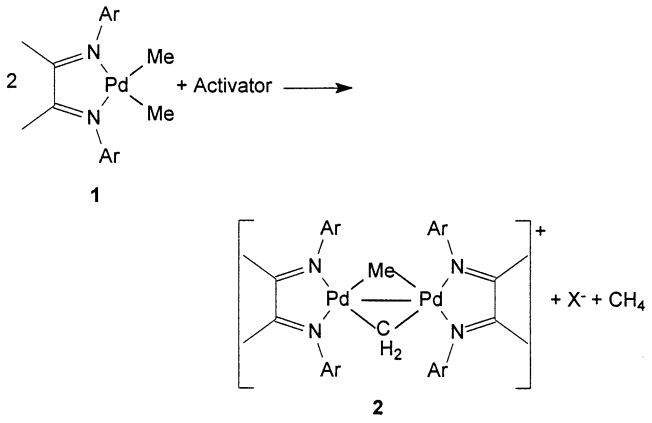

Essentially the same set of α-diimine−Pd complex ^{1}H resonances was also observed with the trityl reagent; the absence of the resonance of $[BMe(C_6F_5)_3]^-$ and the presence of the resonances of 1,1,1-triphenylethane were the only differences. Furthermore, when only 0.5 equiv of either of the trityl activators was added to **1**, the same α-diimine−Pd product was obtained in ∼90% isolated yield. These observations led to the hypothesis that a bis(α-diimine−Pd) species was being formed, and this was confirmed by an electrospray mass spectrum of an aliquot taken from a reaction mixture. The mass spectrum clearly exhibited a molecular ion base peak of *m*/*z* 1051.72, corresponding to a molecular formula of $C_{58}H_{85}N_4Pd_2$ (calculated mass 1051.09 amu) and with an isotope distribution pattern identical with that calculated for $C_{58}H_{85}N_4Pd_2$ (Figure 3). A dipalladium complex could result if units of **1** and $\mathbf{1}^+$ were to combine, possibly as in Scheme 2, to give the cationic complex $[(N\wedge N)Pd(\mu\text{-Me})(\mu\text{-}CH_2)Pd(N\wedge N)]^+$ (**2**). The molecular formula of **2** is precisely $C_{58}H_{85}N_4Pd_2$, and the structure of this unusual μ-Me, μ-CH_2 species was confirmed by X-ray crystallography and by NMR spectroscopy.

The ^{1}H and ^{13}C NMR chemical shifts and assignments of analytically pure **2** are given in the Experimental Section. A variable-temperature ^{1}H NMR study (−90 to 25 °C) indicated that **2** is symmetrical about the two bridging units at temperatures as low as −90 °C, and at no temperature was there evidence of a hydride resonance. While assignments of the α-diimine ^{1}H and ^{13}C resonances are routine,[1a] unambiguous assignments of the μ-CH_2 and μ-CH_3 ^{1}H and ^{13}C resonances were made using 2D ^{1}H−^{13}C HSQC (heteronuclear single quantum coherence) and ^{1}H−^{13}C HMBC (heteronuclear multiple bond coherence) methodologies. The ^{13}C NMR resonance at δ 129.74 correlates with the ^{1}H NMR two-hydrogen resonance at δ 5.72, while the ^{13}C NMR resonance at δ −46.44 correlates with the three-hydrogen ^{1}H NMR resonance at δ 0.04. The latter resonance also shows a very weak long-range correlation (HMBC) to the protons with a chemical shift of δ 5.72. A ^{1}H−^{13}C HSQC DEPT experiment confirmed that the resonances at δ 129.74 and −46.44 are to be assigned to methylene and methyl groups, respectively, consistent with the integrations of the resonances in the ^{1}H NMR spectrum. Interestingly, both the methyl (δ 0.04) and the methylene (δ 5.72) resonances exhibit through-space ^{1}H−^{1}H NOESY correlations to the isopropyl methyl protons of the α-diimine ligands, providing further evidence for the structure proposed in Scheme 2.

The ^{1}H and ^{13}C NMR chemical shifts of δ 5.72 and 129.74 are consistent with a μ-methylene group bridging a species with a metal−metal bond; typical ^{1}H and ^{13}C NMR chemical shifts for this type of structure occur in the ranges δ 5−11 and 110−210, respectively.[9] Furthermore, the highly shielded methyl resonance (δ −46.44) finds precedent in the metal−metal-bonded complexes $(Me_3P)_3Ru(\mu\text{-}CH_2)_2(\mu\text{-Me})Ru(PMe_3)_3$[10] and

(9) (a) Herrmann, W. A. *Adv. Organomet. Chem.* **1982**, *20*, 159. (b) Casey, C. P.; Audett, J. D. *Chem. Rev.* **1986**, *86*, 339. (c) Puddephatt, R. J. *Polyhedron* **1988**, *7*, 767.

(10) Hursthouse, M. B.; Jones, R. A.; Malik, K. M. A.; Wilkinson, G. *J. Am. Chem. Soc.* **1979**, *101*, 4128.

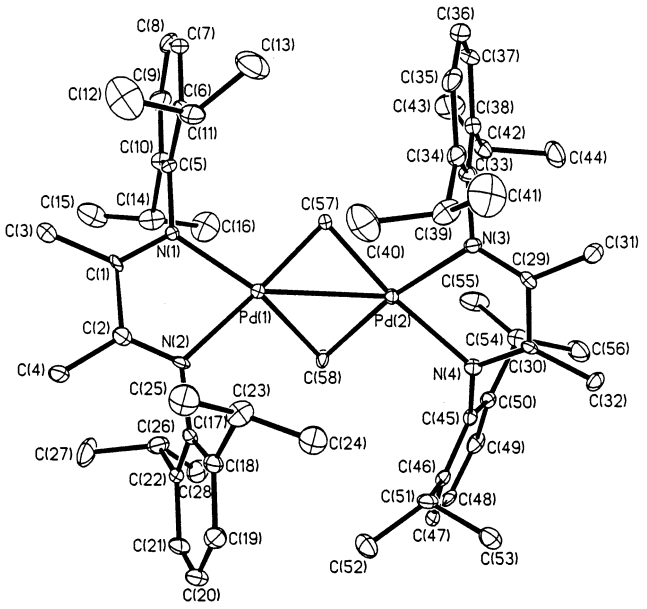

Figure 4. ORTEP plot of $[Pd_2(\mu\text{-}CH_2)(\mu\text{-}Me)(N\wedge N)_2][CF_3SO_3]$ (**2-C**) (30% thermal ellipsoids). The hydrogen atoms and the $[CF_3SO_3]^-$ anion are omitted for clarity. Only one position of the disorder at C(24) and C(25) is shown.

$HOs_3(CO)_{10}(CH_3)$,[11] which exhibit μ-methyl ^{13}C NMR chemical shifts of δ −27.1 and −59.2, respectively.

In an attempt to further define the bonding of the μ-CH_2 and μ-CH_3 groups with the palladium atoms, $^1J_{C-H}$ coupling constants were determined using a 2D $^1H-^{13}C$ HSQC coupled NMR experiment. The μ-CH_3 $^1J_{C-H}$ coupling constant was found to be 131 Hz, a value inconsistent with a static agostic C−H−M interaction which would be expected to result in a $^1J_{C-H}$ coupling in the range 60−90 Hz.[12] Given the above-mentioned symmetry about the Pd−Pd unit, either the μ-CH_3 group is bonded symmetrically or there is a very rapid equilibration of the μ-CH_3 group in solution between the two palladium atoms. The μ-CH_2 resonance exhibits a $^1J_{C-H}$ coupling constant of 141 Hz, a normal value for a μ-CH_2 group in a metal−metal-bonded system.[9]

Crystals of the triflate salt **2-C** suitable for single-crystal X-ray diffraction were obtained, and the structure was determined at 100 K; the molecular structure of the dinuclear cation is shown in Figure 4, while selected bond lengths and angles are listed in Table 1. As can be seen, the structure consists of two Pd(N∧N) units linked by a Pd−Pd bond (2.6987(6) Å) and two bridging carbon atoms. One of the bridging carbon atoms (C(57)) is bound symmetrically with the bond distances Pd(1)−C(57) = 1.982(6) Å and Pd(2)−C(57) = 2.022(6) Å, consistent with a μ-CH_2 linkage.[9] The other bridging carbon (C(58)) is bound asymmetrically (Pd(1)−C(58) = 2.256(6) Å, Pd(2)−C(58) = 2.154(6) Å), with distances slightly longer than in related α-diimine Pd−CH_3 compounds[3b] and is presumably the μ-CH_3 carbon. Although low-temperature (100 K) diffraction data unfortunately did not allow for refinement from the electron density maps of the hydrogen atoms on either of these carbon atoms, the asymmetry of C(58) is consistent with the μ-methyl group being agostically bound through a Pd−C−H−Pd linkage.

Table 1. Selected Bond Lengths (Å) and Angles (deg) in 2-C

Bond Distances			
Pd(1)−Pd(2)	2.6987(6)	Pd(2)−N(3)	2.093(5)
Pd(1)−N(1)	2.081(4)	Pd(2)−N(4)	2.180(4)
Pd(1)−N(2)	2.180(5)	Pd(2)−C(57)	2.022(6)
Pd(1)−C(57)	1.982(6)	Pd(2)−C(58)	2.154(6)
Pd(1)−C(58)	2.256(6)		

Bond Angles			
N(1)−Pd(1)−N(2)	75.19(18)	N(3)−Pd(2)−N(4)	75.95(16)
C(57)−Pd(1)−C(58)	87.0(3)	C(57)−Pd(2)−C(58)	88.9(3)
C(57)−Pd(1)−N(1)	101.4(2)	N(3)−Pd(2)-C(58)	170.9(2)
C(57)−Pd(1)−N(2)	171.1(3)	C(57)−Pd(2)−N(4)	170.1(2)
N(1)−Pd(1)−C(58)	154.2(2)	C(58)−Pd(2)−N(4)	95.0(2)
N(2)−Pd(1)−C(58)	99.6(2)C	C(57)−Pd(1)−Pd(2)	48.25(17)
Pd(1)−C(57)−Pd(2)	84.8(2)	C(58)−Pd(1)−Pd(2)	50.59(16)
Pd(2)−C(58)−Pd(1)	75.4(2)	C(57)−Pd(2)−Pd(1)	46.99(17)
C(57)−Pd(2)−N(3)	100.1(2)	C(58)−Pd(2)−Pd(1)	54.00(16)

The geometry around Pd(2) is nearly square planar, with an angle of 9.2(2)° between the C(57)−C(58)−Pd(2) and the Pd(2)−N(3)−N(4) planes. In contrast, Pd(1) is clearly not square planar, as an angle of 27.5(3)° is formed between the N(1)−N(2)−Pd(1) and the Pd(1)−C(57)−C(58) planes. Interestingly, C(57) (μ-CH_2) is 0.286(9) Å below the Pd(1)−N(1)−N(2) plane, while C(58) (μ-CH_3) is above this plane by 0.972(9) Å. The angle between the Pd(1)−C(57)−C(58) and Pd(2)−C(57)−C(58) planes is 53.2(2)°. The Pd(1)−C(57)−Pd(2) angle of 84.8(2)° is somewhat less acute than those of most other μ-CH_2 complexes with metal−metal bonds (normal range 75−78°),[9] but complexes containing a μ-CH_2 unit without a metal−metal bond tend to have M−C−M angles in the range 89−123° and metal−metal distances in the range 2.84−3.8 Å.[9c] Complex **2-C** falls outside of these parameters, indicating that a metal−metal interaction probably exists. The Pd−Pd bond distance of 2.6987(6) Å is similar to those of the complexes $Pd_2(\mu\text{-dpm})_2(SnCl_3)Cl$ (dpm = bis(diphenylphosphino)methane) (2.644 Å),[13a] $Pd_2(\mu\text{-dpm})_2Br_2$ (2.699 Å),[13b] and [Pd(dippe)(μ-CO)Pd(dippe)Me][BAr′$_4$] (dippe = 1,2-bis(diisopropylphosphino)ethane) (2.6886 Å)[13c] but significantly shorter than that of the μ-CH_2 complex $Pd_2Cl_2(\mu\text{-}CH_2)(\mu\text{-dpm})_2$, which does not contain a Pd−Pd bond (Pd−Pd = 3.171(2) Å).[14]

Previous reports have demonstrated similar bridging arrangements between two metal systems and offer a reasonable comparison to **2**.[10,15,16] Grubbs et al. have reported a Ti/Pt heterobimetallic species with a Ti−Pt bond and μ-CH_3 and μ-CH_2 groups.[15] In the X-ray crystal structure of this complex it was possible to refine the position of the hydrogen atoms on the bridging methyl, indicating a hydrogen agostically bound to the titanium.[15] Bond lengths (Ti−μ-Me = 2.395(8) Å, Pt−μ-Me = 2.122(8) Å) and angles (Ti−Me−Pt 75.6(2)°) similar to those of complex **2-C** were observed. The different

(11) Calvert, R. B.; Shapley, J. R. *J. Am. Chem. Soc.* **1978**, *100*, 6544.
(12) Brookhart, M.; Green, M. L. H.; Wong, L. L. *Prog. Inorg. Chem.* **1988**, *36*, 1.
(13) (a) Olmstead, M. M.; Benner, L. S.; Hope, H.; Balch, A. L. *Inorg. Chim. Acta* **1979**, *32*, 193. (b) Holloway, R. G.; Penfold, B. R.; Colton, R.; McCormick, M. J. *J. Chem. Soc., Chem. Commun.* **1976**, 485. (c) Fryzuk, M. D.; Clentsmith, G. K. B.; Rettig, S. J. *J. Chem. Soc., Dalton Trans.* **1998**, 2007.
(14) Klopfenstein, S. R.; Kluwe, C.; Kirschbaum, K.; Davies, J. A. *Can. J. Chem.* **1996**, *74*, 2331.
(15) Ozawa, F.; Park, J. W.; Mackenzie, P. B.; Schaefer, W. P.; Henling, L. M.; Grubbs, R. H. *J. Am. Chem. Soc.* **1989**, *111*, 1319.
(16) White, S.; Kalberer, E. W.; Bennett, B. L.; Roddick, D. M. *Organometallics* **2001**, *20*, 5731.

Scheme 3. Possible Sequence of Steps for the Formation of 2

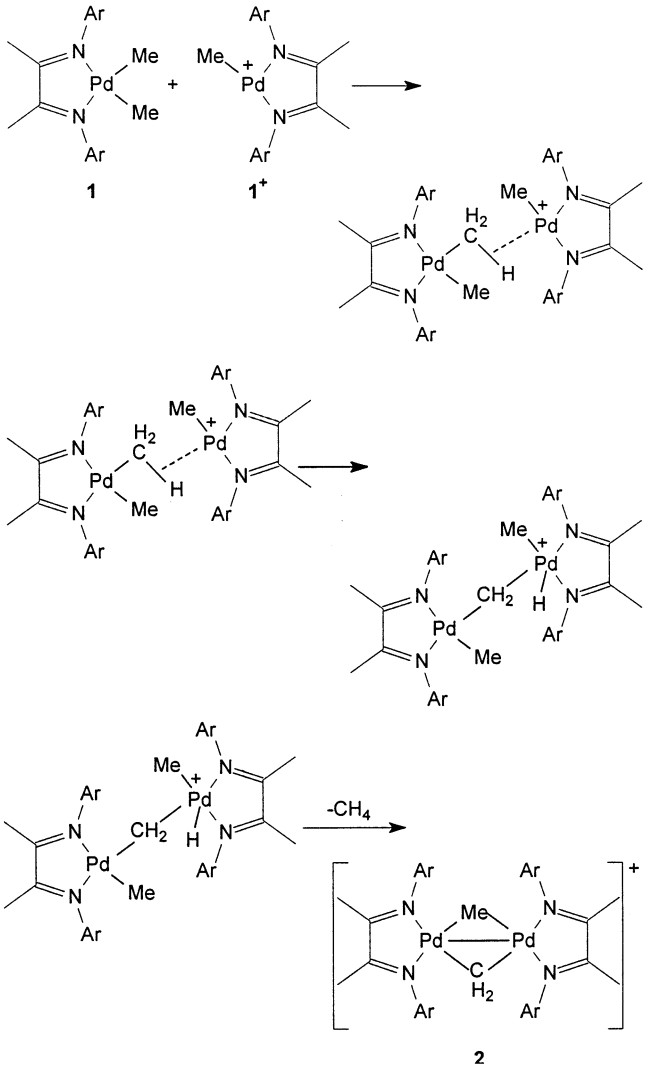

bond lengths between the shorter Pt−Me bond and the longer Ti−Me bond are very similar to the different bond lengths between Pd(1)−C(58) and Pd(2)−C(58), indicating the possible presence of an agostic metal−hydrogen bond in **2-C**.

Wilkinson et al. reported the diruthenium species $(Me_3P)_3Ru(\mu\text{-}CH_2)_2(\mu\text{-}Me)Ru(PMe_3)_3$, in which μ-methyl and μ-methylene groups bridge two ruthenium atoms having a metal−metal bond.[10] This complex has a similar metal−metal bond distance (Ru−Ru = 2.732(1) Å) and bond lengths (Ru−CH_3 = 2.090(7) Å and Ru−CH_2 = 2.109(7) Å) and angles (Ru−CH_3−Ru = 81.6(4)° and Ru−CH_2−Ru = 80.8(4)°) for the bridging groups, as observed in **2-C**. Roddick et al. have recently reported a Pt complex containing a bridging ethylidene.[16] This compound contains a Pt−Pt bond distance of 2.6540(8) Å, which is marginally shorter than the Pd−Pd distance in **2-C**. This slightly shorter distance is expected when comparing Pt and Pd complexes, due to the slightly smaller Pt radius. The distances from Pt to the ethylidene bridging carbon are similar to those in **2-C**.

A possible route by which the dipalladium species **2** may form is shown in Scheme 3; the sequence is related to a general mechanism for alkane C−H activation in α-diimine platinum complexes.[17] A cationic palladium species, $\mathbf{1}^+$ coordinates to **1** via activation of a methyl C−H bond of **1**. This is followed by hydride transfer to the metal, resulting in a palladium bound through a bridging methylene to the second palladium. Reductive elimination of methane would then be followed by coordination of the methyl group from the second palladium to give the final product, **2**. A similar observation has been made by Bochmann et al., who have reported the formation of a μ-CH_3, μ-CH_2 dinuclear zirconium complex by methane loss after methide abstraction using $[Ph_3C][B(C_6F_5)_4]$.[18]

Generation of conventional mononuclear, catalytically active, cationic complexes of the type $[PdMe(S)(N\wedge N)]^+$ is typically achieved via procedures different from those used in this study. Brookhart and others generally synthesize the cationic palladium species in one of two ways, via removal of the chloride from $PdMeCl(N\wedge N)$ with an alkali-metal borate salt in a coordinating solvent, S, such as CH_3CN and Et_2O, or via protonation of a methyl group from $PdMe_2(N\wedge N)$ in the same coordinating solvents (eq 1).[1,3b] In both cases a solvent-stabilized, mononuclear cationic species is formed rather than a dipalladium complex such as **2**. In an effort to further understand the relationship between **2** and mononuclear catalysts, we have carried out a ^{1}H NMR experiment in which **1** was activated with $B(C_6F_5)_3$ and $[Ph_3C][B(C_6F_5)_4]$ in the presence of a large excess of ethylene. The deep red **2** appears to be formed initially, as a ^{1}H NMR spectrum run immediately after activation of **1** showed that **2** was present as ∼15% of the total palladium at that point. However, the resonances of **2** disappeared within 10 min as the initially formed orange-yellow color faded to yellow and low-density polyethylene formed (see below). In a complementary NMR experiment, preformed **2** was treated with a smaller excess of ethylene and found to convert partially to $\mathbf{1}^+$; however, most of the ethylene was polymerized. These experiments demonstrate clearly that the dinuclear **2** reacts with ethylene and converts to the mononuclear catalytic complex $\mathbf{1}^+$. While catalytic activity of **2** cannot be ruled out, the fact the polyethylene formed is identical with that formed utilizing the mononuclear catalyst seems to rule out catalysis by **2**.

Polymerization Reactions. For purposes of comparison, polymerizations by **1** activated with $B(C_6F_5)_3$, $[Ph_3C][B(C_6F_5)_4]$, and $[Ph_3C][CF_3SO_3]$ were performed in dichloromethane at 25 ± 2 °C under 1 atm of ethylene. In a general procedure, the catalyst precursor **1** was dissolved in CH_2Cl_2 which had been saturated with ethylene and then activated by addition of a methide abstracting agent. In each case the solutions turned from the deep red-brown of **1** to light yellow. Polymerizations were run for varying periods of time before being quenched with methanol. The solvents were removed from the reaction mixtures under reduced pressure, and the crude polymers were dissolved in hexanes and the solutions passed through silica gel to remove catalyst. The hexanes were then removed under reduced pressure to leave colorless, viscous polymeric materials. Information concerning conditions of the

(17) (a) Zhong, H. A.; Labinger, J. A.; Bercaw, J. E. *J. Am. Chem. Soc.* **2002**, *124*, 1378 and references therein. (b) Labinger, J. A.; Bercaw, J. E. *Nature* **2002**, *417*, 507.

(18) Bochmann, M.; Cuenca, T.; Hardy, D. T. *J. Organomet. Chem.* **1994**, *484*, C10.

Table 2. Polymerization Results

expt	cat.	amt of (N∧N)PdMe$_2$ (mg, μmol)	amt of activator (mg, μmol)	time (h)	yield (g)	activity (kg of PE (mol of cat.$^{-1}$ h^{-1})	$10^{-3}M_w$	$10^{-3}M_n$	M_w/M_n	branches per 1000 C
1	**1-A**	15.0, 27.7	14.9, 29.1	0.5	1.06	77	31	27	1.13	91
2	**1-A**	16.2, 29.9	16.1, 31.4	1	2.24	75	54	43	1.25	98
3	**1-A**	15.2, 28.1	15.1, 29.5	1.5	2.64	63	70	59	1.19	97
4	**1-B**	14.0, 25.9	25.1, 27.2	0.5	1.14	88	27	23	1.17	104
5	**1-B**	14.8, 27.4	26.5, 28.8	1	2.19	80	77	65	1.18	99
6	**1-B**	14.6, 27.0	26.1, 28.4	1.5	2.89	71	94	79	1.18	90
7	**1-C**	13.4, 24.8	10.2, 26.0	0.5	0.87	70	9.5	4.7	1.5	100
8	**1-C**	14.6, 27.0	11.1, 28.4	1	1.66	61	9.3	4.1	2.27	90
9	**1-C**	16.3, 30.1	12.4, 31.6	1.5	2.36	52	9.3	4.9	1.91	98

polymerization experiments, conversions, and polymer molecular weight data (GPC) are summarized in Table 2.

The ^{1}H and ^{13}C{^{1}H} NMR spectra ($CDCl_3$) of the polymers formed by all three catalysts were essentially identical with each other and with those of the highly branched, low-density polyethylene formed by activation of **1** by $[H(Et_2O)_2][B\{3,5\text{-}C_6H_3(CF_3)_2\}_4]$.[1a] Thus, the catalytically active species investigated here are presumably identical both with each other and with the well-studied catalyst containing the $[B\{3,5\text{-}C_6H_3(CF_3)_2\}_4]^-$ counteranion.[1a]

As can be seen from Table 2, activities of catalysts **1-A** and **1-B** and the molecular weights of the polymers obtained from **1-A** and **1-B** vary only slightly, while the activities of catalyst **1-C** are somewhat lower and the molecular weights of its polymers are significantly lower. Thus, as anticipated, the most weakly coordinating anion, $[B(C_6F_5)_4]^-$, exhibits the highest activities and produces the highest molecular weights, while the most coordinating anion, triflate,[19] has the lowest. All three systems show a decrease in activity with time, which can presumably be attributed to catalyst decomposition, although the activities of the catalysts relative to each other remain approximately constant with time. The differences in activities are much smaller than those observed in early-metallocene-based systems using the $[BMe(C_6F_5)_3]^-$ and $[B(C_6F_5)_4]^-$ anions, where variations as large as an order of magnitude have been observed for activities in zirconocene systems.[20]

It was found that the molecular weights of the polymers produced by catalysts **1-A** and **1-B**, which contain the more weakly coordinating anions $[BMe(C_6F_5)_3]^-$ and $[B(C_6F_5)_4]^-$, increased with time (Table 2, experiments 1−6), while those produced by **1-C** ($[CF_3SO_3]^-$) remained essentially constant with time (Table 2, experiments 7−9). In addition to the increase in molecular weight with time, low polydispersities were also observed for the $[BMe(C_6F_5)_3]^-$ and $[B(C_6F_5)_4]^-$ systems. The behaviors of **1-A** and **1-B** thus implied the existence of living polymers, as has been observed with similar Pd α-diimine complexes.[21]

Returning to **2**, examination of the structure suggests that a potential vacant site is present if an agostic interaction exists between one Pd and the bridging methyl group. Bulk polymerization of ethylene using **2-A** was carried out, and it was found that addition of ethylene to a solution of this catalyst resulted in the formation of polyethylene with an activity of 97 kg of PE (mol of catalyst)$^{-1}$ h^{-1}, assuming that **2-A** forms only 1 mol of mononuclear catalyst. The polymer formed had a microstructure identical with those produced in experiments 1−9 (Table 2) using $\mathbf{1}^+$, as well as similar molecular weights and a similar polydispersity index as compared to the PE produced by **1-A** (30 min: M_n = 36 000, M_w/M_n = 1.15). The NMR experiments described above, in which **1** was activated with $B(C_6F_5)_3$ and $[Ph_3C][B(C_6F_5)_4]$ in the presence of a large excess of ethylene and in which preformed **2** was exposed to lesser amounts of ethylene, suggest strongly not only that coordination of the ethylene inhibits the initial formation of the dinuclear species **2** but also that the latter reacts with ethylene to form the mononuclear catalyst. It thus seems that **2** is not the active catalyst during the polymerization of ethylene by this catalyst system but, rather, represents a high-energy resting state associated with the catalytic system. We do not know at this point if the μ-CH_2 and the μ-CH_3 groups are incorporated into the polymer.

Summary. The compound $PdMe_2(N\wedge N)$ ($N\wedge N$ = ArN═CMeCMe═NAr, Ar = 2,6-$C_6H_3(i\text{-}Pr)_2$) reacts with the methide abstractors $B(C_6F_5)_3$, $[Ph_3C][B(C_6F_5)_4]$, and $[Ph_3C][CF_3SO_3]$ in the absence of ethylene to give the metal−metal-bonded, dinuclear, cationic complex $[(N\wedge N)Pd(\mu\text{-}CH_2)(\mu\text{-}Me)Pd(N\wedge N)]^+$, with bridging methylene and methyl units. This complex is characterized by ^{1}H and ^{13}C{^{1}H} NMR spectroscopy, mass spectrometry, and X-ray crystallography and is found to react with ethylene to form the same type of low-density polyethylene produced by the mononuclear catalysts formed by methide abstraction from $PdMe_2(N\wedge N)$ by $B(C_6F_5)_3$, $[Ph_3C][B(C_6F_5)_4]$, $[Ph_3C][CF_3SO_3]$, and $[H(Et_2O)_2][B\{3,5\text{-}C_6H_3(CF_3)_2\}_4]$. NMR experiments suggest strongly that the dinuclear complex converts to a catalytic monomethyl palladium complex on reaction with ethylene and is a previously unknown, high-energy species associated with the catalytic cycle.

The same cationic monomethyl palladium species appear to be the catalyst involved with all four anions, and the three weakly coordinating counteranions $[BMe(C_6F_5)_3]^-$, $[B(C_6F_5)_4]^-$, and $[B\{3,5\text{-}C_6H_3(CF_3)_2\}_4]^-$ differ little in their effects on the polymerization process. These results are consistent with the resting state for all three systems being the cationic ethylene complex $[Pd(\eta^2\text{-}C_2H_4)(\sim\text{polymer})(N\wedge N)]^+$ and are in contrast with metallocene catalysts of the group 4 metals, where the nature of the counteranions has a major impact on the polymerization process. Interestingly, activation by $[Ph_3C][CF_3SO_3]$ gives a catalyst of considerably reduced potency, suggesting that the triflate anion is a better

(19) For evidence that triflate is a better coordinating ligand than, for example, $[B(C_6H_5)_4]^-$, see: (a) Linert, W.; Jameson, R. F.; Taha, A. *J. Chem. Soc., Dalton Trans.* **1993**, 3181. (b) Linert, W.; Fukuda, Y.; Camard, A. *Coord. Chem. Rev.* **2001**, *218*, 113.

(20) For examples see: Jia, L.; Yang, X.; Stern, C. L.; Marks, T. J. *Organometallics* **1997**, *16*, 842.

(21) Gottfried, A. C.; Brookhart, M. *Macromolecules* **2001**, *34*, 1140.

ligand in this system and does compete effectively for the active site on the metal.

Experimental Section

All experiments were carried out under purified argon using standard Schlenk line techniques or an MBraun Labmaster glovebox. Solvents were purified by standard methods and distilled and degassed before use. Toluene-d_8 and CD_2Cl_2 were dried over Na/benzophenone and CaH_2, respectively, and vacuum-distilled prior to use. All ^1H, $^{13}C\{^1H\}$, and ^{19}F NMR 1D spectra and all 2D COSY, HSQC, HMBC, NOESY, and HSQC DEPT spectra (used for assignment and structural determination) were run on Bruker AC 200 and Bruker Avance 400 spectrometers operating at 200 and 400 MHz, respectively. Chemical shifts are referenced with respect to internal TMS using residual proton or carbon resonances of the solvents for ^1H and $^{13}C\{^1H\}$ spectra and external $CFCl_3$ for ^{19}F studies. GPC data were obtained using a Waters Associates Model GPC-2690 liquid chromatograph with separation columns consisting of cross-linked polystyrene gel (μ-Styragel) with various pore sizes: 100, 500, 1000, 10 000 Å. Calibration of the instrument was performed using polystyrene standards ranging in molecular weights from 2350 g/mol to 2 300 000 g/mol.

All chemicals, except as noted below, were purchased from Aldrich and were purified as appropriate before use. The compounds $B(C_6F_5)_3$,[22] $[Ph_3C][CF_3SO_3]$,[23] H_2PdCl_4,[24] $CODPdCl_2$,[25] $CODPdMe_2$,[26] (N∧N)$PdMe_2$ (**1**),[1a] and *N*,*N*′-bis(2,6-diisopropylphenyl)-1,4-diazabutadiene[27] were synthesized according to literature procedures. $[Ph_3C][B(C_6F_5)_4]$ was purchased from Asahi Glass Company Ltd., Tokyo. Polymerization grade ethylene (99%+ purity) was purchased from Air Products and was dried prior to use by passage through a column (3′ × 1″) of 4A molecular sieves which had been dried under reduced pressure while being heated above 100 °C and then cooled to room temperature and purged with ethylene for 15 min prior to use.

NMR-Scale Reaction of 1 and $B(C_6F_5)_3$. In an NMR tube, 10.0 mg of **1** (18.5 μmol) and 10.0 mg of $B(C_6F_5)_3$ (19.5 μmol) were dissolved in 0.5 mL of CD_2Cl_2, resulting in some effervescence and the formation of a deep red solution. A ^1H NMR spectrum run immediately exhibited the following resonances (25 °C, CD_2Cl_2): δ 7.22−7.10 (12H, m), 5.71 (2H, s), 2.77 (4H, sept, $^3J_{H-H}$ = 6.8 Hz), 2.60 (4H, sept, $^3J_{H-H}$ = 6.8 Hz), 2.02 (6H, s), 1.95 (6H, s), 1.12 (12H, d, $^3J_{H-H}$ = 6.8 Hz), 1.06 (36H, d, $^3J_{H-H}$ = 6.8 Hz), 0.46 (3H, br s), 0.04 (3H, s), 0.21 (s, C*H*$_4$). The same spectrum was produced when only half the amount of $B(C_6F_5)_3$ was added. The ^{19}F NMR spectrum exhibited peaks of unreacted $B(C_6F_5)_3$ and of $[BMe(C_6F_5)_3]^-$. ^{19}F NMR of $B(C_6F_5)_3$ (25 °C, CD_2Cl_2): δ −129.1 (2F, br s, *o*-C_6F_5), −144.7 (1F, br s, *p*-C_6F_5), −162.0 (2F, br s, *m*-C_6F_5). ^{19}F NMR of $[BMe(C_6F_5)_3]^-$ (25 °C, CD_2Cl_2): δ −134.27 (2F, d, $^3J_{F-F}$ = 20.3 Hz, *o*-C_6F_5), −166.45 (1F, t, $^3J_{F-F}$ = 20.7 Hz, *p*-C_6F_5), −169.02 (2F, t, $^3J_{F-F}$ = 21.4 Hz, *m*-C_6F_5).

NMR-Scale Reaction of 1 and $[Ph_3C][B(C_6F_5)_4]$. In an NMR tube 6.1 mg of **1** (11.3 μmol) and 10.4 mg of $[Ph_3C][B(C_6F_5)_4]$ (11.3 μmol) were dissolved in 0.5 mL of CD_2Cl_2, resulting in some effervescence and the formation of a deep red solution. A ^1H NMR spectrum was recorded immediately and was found to be identical with that observed above with trityl resonances substituted for that of $[BMe(C_6F_5)_3]^-$. The methane resonance at δ 0.21 was again present. In addition, peaks for unreacted trityl borate and 1,1,1-triphenylethane were observed. The same product was synthesized when only half the amount of $[Ph_3C][B(C_6F_5)_4]$ was added. ^1H NMR of Ph_3CCH_3 (25 °C, CD_2Cl_2): δ 2.17 (3H, s) [C*H*$_3$], peaks in the aromatic region overlap with those of **2**. ^1H NMR of $[Ph_3C][B(C_6F_5)_4]$ (25 °C, CD_2Cl_2): δ 8.27 (1H, t, $^3J_{H-H}$ = 7.2 Hz, *p*-C_6H_5), 7.88 (2H, t, $^3J_{H-H}$ = 8.2 Hz, *m*-C_6H_5), 7.66 (2H, d, $^3J_{H-H}$ = 8.0 Hz, *o*-C_6H_5).

Reaction of 1.0 equiv of 1 with 0.5 equiv of $B(C_6F_5)_3$. In a Schlenk flask, 58.3 mg of **1** (108 μmol) and $B(C_6F_5)_3$ (27.6 mg, 53.9 μmol) were dissolved in 1.5 mL of CH_2Cl_2, resulting in some effervescence and the formation of a deep red solution. The CH_2Cl_2 solution was layered with 10 mL of pentanes and cooled to −30 °C, yielding dark red crystals. The solvent was removed by decantation, and the crystals were washed three times with 3 mL of pentane to leave deep red crystals of **2-A** (77.5 mg, 91% yield). ^1H NMR (25 °C, CD_2Cl_2): δ 7.22−7.10 (12H, m, N(C_6H_3)), 5.71 (2H, s, μ-CH_2), 2.77 (4H, sept, $^3J_{H-H}$ = 6.8 Hz, C*H*(CH$_3$)$_2$), 2.60 (4H, sept, $^3J_{H-H}$ = 6.8 Hz, C*H*(CH$_3$)$_2$), 2.02 (6H, s, NC(C*H*$_3$)), 1.95 (6H, s, NC(C*H*$_3$)), 1.12 (12H, d, $^3J_{H-H}$ = 6.8 Hz, CH(C*H*$_3$)$_2$), 1.06 (36H, d, $^3J_{H-H}$ = 6.8 Hz, CH(C*H*$_3$)$_2$), 0.46 (3H, br s, C*H*$_3$B$(C_6F_5)_3^-$), 0.04 (3H, s, μ-C*H*$_3$). $^{13}C\{^1H\}$ NMR (25 °C, CD_2Cl_2): δ 173.58, 171.09 (N=*C*(CH$_3$)-*C*′(CH$_3$)=N), 144.98, 141.00 (Ar, Ar′: C_{ipso}), 137.79, 137.25 (Ar, Ar′: C_o), 129.74 (μ-*C*H$_2$), 127.57, 127.30 (Ar, Ar′: C_p), 124.23 (Ar, Ar′: C_m), 28.91 (*C*H(CH$_3$)$_2$), 28.65 (*C*′H(CH$_3$)$_2$), 23.98, 23.92, 23.78, 23.57 (CH(*C*H$_3$)(*C*′H$_3$) and C′H(*C*H$_3$)(*C*′H$_3$)), 20.63, 20.21 (N=C(*C*H$_3$)C′(*C*′H$_3$)=N), −46.44 (μ-*C*H$_3$). ^{19}F NMR (25 °C, CD_2Cl_2): δ −134.27 (2F, d, $^3J_{F-F}$ = 20.3 Hz, *o*-C_6F_5), −166.45 (1F, t, $^3J_{F-F}$ = 20.7 Hz, *p*-C_6F_5), −169.02 (2F, t, $^3J_{F-F}$ = 21.4 Hz, *m*-C_6F_5). ESMS (*m*/*z* (relative intensity)): positive ions 1059.70 (1.2), 1058.70 (4.1), 1057.71 (10.4), 1056.71 (16.7), 1055.72 (33.5), 1054.71 (36.9), 1053.72 (75.8), 1052.71 (71.5), 1051.72 (100), 1050.72 (85.4), 1049.72 (87.7), 1048.71 (74.6), 1047.72 (55.3), 1046.72 (23.3), 1045.71 (7.9), 1044.72 (2.2), 539.16 (5.0), 538.15 (8.1), 511.15 (13.8), 509.18 (19.9), 507.16 (15.8), 506.16 (9.4), 505.18 (5.0), 405.34 (8.0); calcd positive ions for $C_{58}H_{85}N_4Pd_2$ 1059.50 (1.2), 1058.49 (4.3), 1057.49 (10.0), 1056.49 (17.0), 1055.49 (33.4), 1054.49 (38.7), 1053.49 (74.5), 1052.49 (70.0), 1051.49 (100), 1050.49 (84.5), 1049.49 (85.8), 1048.49 (73.8), 1047.49 (53.5), 1046.49 (21.9), 1045.49 (7.5), 1044.49 (2.1); negative ions 528.98 (2.6), 528.01 (21.1), 527.03 (100), 525.98 (25.6); calcd negative ions for $C_{19}H_3F_{15}B$ 529.02 (2.1), 528.01 (20.6), 527.01 (100), 526.01 (23.6). Anal. Found for $C_{77}H_{88}BF_{15}N_4Pd_2$: C, 58.27; H, 5.84; N, 3.46. Calcd: C, 58.60; H, 5.62; N, 3.55.

Reaction of 1.0 equiv of 1 and 0.5 equiv of $[Ph_3C][B(C_6F_5)_4]$. By a procedure identical with that used in the synthesis of complex **2-A**, 35.6 mg of **1** (65.7 μmol) and 30.3 mg of $[Ph_3C][B(C_6F_5)_4]$ (32.9 μmol) were dissolved in 1.5 mL of CH_2Cl_2 in a Schlenk flask and layered with 10 mL of pentanes and cooled to −30 °C, yielding dark red crystals. The product was isolated as deep red crystals of **2-B** (53.8 mg, 94% yield). ^1H NMR (25 °C, CD_2Cl_2): cation peaks identical with those of complex **2-A**. ^{19}F NMR (25 °C, CD_2Cl_2): δ −134.19 (2F, br s, *o*-C_6F_5), −164.87 (1F, t, $^3J_{F-F}$ = 21.1 Hz, *p*-C_6F_5), −168.69 (2F, t, $^3J_{F-F}$ 16.2 Hz, *m*-C_6F_5). Anal. Found for $C_{82}H_{85}BF_{20}N_4Pd_2$: C, 57.03; H, 5.05; N, 3.17. Calculated: C, 56.92; H, 4.95; N, 3.24.

Reaction of 1.0 equiv of 1 and 0.5 equiv of $[Ph_3C][CF_3SO_3]$. By a procedure identical with that used in the synthesis of complex **2-A**, 49.0 mg of **1** (90.6 μmol) and 17.8 mg of $[Ph_3C][CF_3SO_3]$ (45.3 μmol) were dissolved in 1.5 mL of CH_2Cl_2 in a Schlenk flask and layered with 10 mL of pentanes and cooled to −30 °C, yielding dark red crystals. **2-C** was isolated as a deep red crystalline material suitable for single-crystal X-ray diffraction (48.2 mg, 89% yield). ^1H NMR (25 °C, CD_2Cl_2): cation peaks identical with those of complex **2-A**. ^{19}F

(22) Pohlmann, J. L.; Brinckmann, F. E. *Z. Naturforsch., B* **1965**, *20b*, 5.
(23) Forbus, T. R., Jr.; Martin, J. C. *J. Org. Chem.* **1979**, *44*, 313.
(24) Kauffman, G. B.; Tsai, J. H. S. *Inorg. Synth.* **1966**, *8*, 234.
(25) Drew, D.; Doyle, J. R. *Inorg. Synth.* **1972**, *13*, 47.
(26) Rudler-Chauvin, M.; Rudler, H. *J. Organomet. Chem.* **1977**, *134*, 115.
(27) tom Dieck, H.; Svoboda, M.; Greiser, T. *Z. Naturforsch., B* **1981**, *36b*, 823.

NMR (25 °C, CD_2Cl_2): δ 90.06. Anal. Found for $C_{59}H_{85}F_3N_4O_3Pd_2S$: C, 59.14; H, 7.24; N, 4.69. Calcd: C, 59.04; H, 7.14; N, 4.67.

General Polymerization Procedures. Compound **1** (∼15.0 mg, ∼28 μmol) was dissolved in 10 mL of CH_2Cl_2, and the resulting deep red-brown solution was saturated with ethylene for 10 min by bubbling ethylene through the stirred solution. To this solution was then added a solution of 1.05 equiv of activator (∼30 μmol) in 10 mL of CH_2Cl_2, resulting in the formation of a clear yellow solution. Ethylene was continually bubbled through the solution for the length of the polymerization (0.5, 1.0, or 1.5 h), at which point polymerization was quenched by the addition of ∼20 mL of methanol. The reaction temperature was monitored using a thermocouple immersed into the polymerization solution, and the temperature was maintained at 25 ± 2 °C by cooling in a water bath. The solvent was removed from the crude polymer solution under reduced pressure to leave a black oily residue, which was dissolved in ∼30 mL of hexanes and eluted through silica gel. The hexanes were removed under reduced pressure to leave a viscous colorless oil. Details of the polymerization experiments are summarized in Table 2.

NMR Study of the Activation of 1.0 equiv of 1 with 1.0 equiv of $B(C_6F_5)_3$ in the Presence of Ethylene. A 7.5 mg portion of **1** (13.8 μmol) in an NMR tube was dissolved in 0.50 mL of CD_2Cl_2 to form a deep red-brown solution. The solution was saturated with ethylene for ∼30 s, and a solution of 7.4 mg of $B(C_6F_5)_3$ (14.5 μmol) in 0.50 mL of CD_2Cl_2 was added to the tube, resulting in the formation of a yellow solution. A ^{1}H NMR spectrum was obtained immediately and exhibited weak resonances of complex **2-A** in addition to new resonances at δ 4.23 (s, ((N∧N)Pd[$(CH_2)_nCH_3$](CH_2═CH_2)) and 2.34 and 2.21 (s, (N═C(CH_3)C′(CH_3)═N). The latter resonances are similar to those observed by Brookhart et al. during low-temperature NMR studies in which ethylene was added to a solution of the cationic species $\mathbf{1}^+$.[1a] A similar reaction of $[Ph_3C][B(C_6F_5)_4]$ with **1** under identical conditions yielded a similar ^{1}H NMR spectrum.

NMR Study of the Reaction of 2-A with Ethylene. To a deep red solution of **2-A** (14.3 mg, 9.06 μmol) in 0.5 mL of CD_2Cl_2 in an NMR tube was added 1.5 mL (∼70 μmol) of ethylene. The tube was shaken, and an ^{1}H NMR spectrum was recorded. Further 1.5 mL aliquots of ethylene were added after 10 and 20 min, the reaction being monitored by ^{1}H NMR spectroscopy. Although the reaction mixture remained red and the resonances of **2-A** were observed throughout the experiment, the resonances decreased in intensity as those of a new species increased in intensity. The resonances of the new complex are consistent with the formation of complex $\mathbf{1}^+$ observed by Brookhart et al.[1a] New peaks: δ 7.45−7.33 (m, Ar′), 2.75 (m, Ar′CH(CH_3)$_2$, overlapped by peak of **2-A**), 2.34 and 2.21 (s, N═C(CH_3)C′(CH_3)═N). Although the resonance of coordinated ethylene was not observed, this is not surprising (see the Supporting Information of ref 1a). The resonances of polyethylene[1a] were observed and increased in intensity after each addition (see below).

Polymerization of Ethylene with 2-A. A 7.5 mg portion of **2-A** (4.75 μmol) was dissolved in 10 mL of CH_2Cl_2 at 25 °C, generating a deep red color. Ethylene was then bubbled through the solution for 30 min and, after ∼5 min, the deep red solution had turned yellow. The reaction was quenched after 30 min with 20 mL of methanol, and the solvent was removed under reduced pressure. The crude polymer was dissolved in 30 mL of hexanes and the solution passed through silica gel, after which the solvent was removed under reduced pressure to yield a clear, colorless, viscous oil (0.23 g). A ^{1}H NMR spectrum was identical with that of the PE produced above. GPC: M_w = 42 000, M_n = 36 000, M_w/M_n = 1.15. Activity: 97 kg of PE (mol of cat.)$^{-1}$ h^{-1}. Branches (per 1000 C): 106.

Table 3. Crystal Data and Data Collection and Structure Refinement Details for 2-C

formula, fw	$C_{59}H_{85}F_3N_4O_3Pd_2S$, 1200.17
temp	100(2) K
wavelength	0.710 73 Å
cryst syst, space group	orthorhombic, $P2_12_12_1$
unit cell dimens	
a	13.0389(8) Å
b	19.0498(14) Å
c	24.5120(17) Å
V, *Z*	6088.5(6) Å^3, 4
cryst color, habit	red, block
density (calcd)	1.309 Mg/m^3
abs coeff	0.678 mm^{-1}
F(000)	2504
cryst size	0.20 × 0.15 × 0.10 mm^3
θ range	1.98−28.29°
index ranges	$-17 \le h \le 16$, $-14 \le k \le 24$, $-31 \le l \le 32$
no. of coll, indep rflns	39 145, 14 268 (R_{int} = 0.0619)
abs cor	SADABS
completeness to θ = 28.29°	97.0%
refinement method	full-matrix least squares on F^2
no. of data/restraints/params	14 268/0/648
goodness of fit on F^2	1.165
final *R* indices[a] ($I > 2\sigma(I)$)	R1 = 0.0652, wR2 = 0.1342
R indices[a] (all data)	R1 = 0.0735, wR2 = 0.1379
abs struct param	0.03(4)
largest diff peak and hole	1.395 and −1.347 e Å^{-3}

[a] R1 = $\sum||F_o| - |F_c||/\sum|F_o|$; wR2 = $\{\sum[w(F_o^2 - F_c^2)^2]/\sum[w(F_o^2)^2]\}^{1/2}$; $w = 1/[\sigma^2(F_o^2) + (aP)^2 + bP]$, $P = [2F_c^2 + \max(F_o,0)]/3$.

Start/Stop/Start Polymerizations. Polymerizations were performed identically with those listed above in the general procedure. At 30 min, an aliquot of the active system was removed from the polymerization reaction and quenched with 10 mL of methanol. The system was purged for 30 min with argon, and then monomer addition was reinitiated by bubbling ethylene through the solution. After a further 30 min, the remaining solution was quenched with 10 mL of methanol. The polymer samples were purified as before. **1-A**: GPC (0.5 h) M_w = 27 000, M_n = 24 000, M_w/M_n = 1.14; GPC (1.0 h) M_w = 54 000, M_n = 46 000, M_w/M_n = 1.18. **1-B**: GPC (0.5 h) M_w = 18 000, M_n = 17 000, M_w/M_n = 1.06; GPC (1.0 h) M_w = 32 000, M_n = 29 000, M_w/M_n = 1.12. The ^{1}H NMR spectra of the polymers were identical with those discussed above.

X-ray Crystal Structure Determination. Diffraction intensity data were collected with a Bruker Smart Apex CCD diffractometer. Crystal data and data collection and refinement parameters are given in Table 3. The space group was determined from systematic absences in the diffraction data. The structure was solved using direct methods, completed by subsequent difference Fourier syntheses, and refined by full-matrix least-squares procedures on reflection intensities (F^2). SADABS absorption corrections were applied (T_{min}/T_{max} = 0.81). All non-hydrogen atoms were refined with anisotropic displacement coefficients. The hydrogen atoms were treated as idealized contributions, except for the H atoms of the bridging μ-CH_2 and μ-CH_3 groups, which were not found on the *F* map and not included in refinement. In the structure of **2-C**, two Me groups (the C(24) and C(25) atoms) and the O(1) and F(1) atoms of the $[CF_3SO_3]^-$ group are disordered on two positions with occupation multiplicity μ = 0.65, 0.35 μ = 0.51, 0.49, and μ = 0.64, 0.36, respectively. Only one position for these atoms is shown in Figure 4. The Flack parameter is 0.03(4); i.e., the given structure corresponds to the absolute structure of **2-C**. All software and source scattering factors are contained in the SHELXTL (version 5.10) program package.[28] The ORTEP plot of **2-C** is shown in Figure 4.[29]

(28) SHELXTL Version 5.10, Crystal Structure Analysis Package; Bruker AXS, Madison, WI, 1998.

(29) Burnett, M. N.; Johnson, C. K. ORTEP-III: Oak Ridge Thermal Ellipsoid Plot Program for Crystal Structure Illustrations; Report ORNL-6895; Oak Ridge National Laboratory, Oak Ridge, TN, 1996.

Acknowledgment. We thank the Government of Ontario (Ontario Graduate Scholarship to J.H.B.), Queen's University (Queen's Graduate Award to J.H.B.), and the Natural Sciences and Engineering Research Council (Research Grant to M.C.B.) for funding this research.

Supporting Information Available: Crystallographic details, including figures of **2-C** showing complete numbering schemes for the cation and anion and a thermal ellipsoid figure and tables of positional and thermal parameters. This material is available free of charge via the Internet at http://pubs.acs.org.

OM020673L